Discovery of Protein Phosphatase 2C Inhibitors by Virtual Screening

Jessica P. Rogers,[†,#] Albert E. Beuscher, IV,[‡,||,#] Marc Flajolet,[†] Thomas McAvoy,[†] Angus C. Nairn,[†,§] Arthur J. Olson,*[,‡] and Paul Greengard*[,†]

Laboratory of Molecular and Cellular Neuroscience, The Rockefeller University, 1230 York Avenue, New York, New York 10021, and Department of Molecular Biology, The Scripps Research Institute, 10550 North Torrey Pines Road, La Jolla, California 92037

Received October 13, 2005

Protein phosphatase 2C (PP2C) is an archetype of the PPM Ser/Thr phosphatases, characterized by dependence on divalent magnesium or manganese cofactors, absence of known regulatory proteins, and resistance to all known Ser/Thr phosphatase inhibitors. We have used virtual ligand screening with the AutoDock method and the National Cancer Institute Diversity Set to identify small-molecule inhibitors of PP2Cα activity at a protein substrate. These inhibitors are active in the micromolar range and represent the first non-phosphate-based molecules found to inhibit a type 2C phosphatase. The compounds docked to three recurrent binding sites near the PP2Cα active site and displayed novel Ser/Thr phosphatase selectivity profiles. Common chemical features of these compounds may form the basis for development of a PP2C inhibitor pharmacophore and may facilitate investigation of PP2C control and cellular function.

Introduction

The reversible phosphorylation of proteins on serine and threonine residues functions as a critical control mechanism in intracellular signal transduction, regulating a wide range of processes from metabolism to cell division to neurotransmission. Protein kinases and protein phosphatases act in dynamic opposition to make and break phosphoester bonds, determining the rate, extent, and persistence of phosphorylation and its associated signal responses.[1,2]

An estimated one-third of human intracellular proteins are subject to regulation by phosphate. Abnormal phosphorylation is known to be either a cause or a consequence of a variety of prominent human diseases including cancer, Alzheimer's disease, chronic inflammatory disease, and diabetes.[3] Both kinases and phosphatases are thus strong potential drug targets. Protein kinases, numbering around 500 in the human genome,[4] are fairly advanced in this respect; they currently form the second largest group of drug targets following the G-protein-coupled receptors (GPCRs), and a number of kinase inhibitors are approved for clinical use or in clinical trials, especially for the treatment of cancer.[5] In contrast, protein phosphatases—around one-fourth the number of kinases in the human genome—have been widely considered as general, negative regulators of kinase activity. Although moderately specific phosphatase inhibitors are emerging for both protein tyrosine[6] and serine/threonine[7] phosphatases, the further design and development of such molecules for basic research and therapeutic use will be important.[8] The work reported here contributes to this effort for a relatively understudied group of Ser/Thr phosphatases.

The Ser/Thr-specific phosphatases are metal-dependent enzymes divided into two major families: the PPP family, which includes protein phosphatases 1, 2A, and 2B (PP1, PP2A, PP2B/calcineurin), and the PPM family, which includes PP2C.[9,10] The PPPs show high homology in their catalytic domains and are subject to complex regulation by associated subunits, which affect targeting and substrate specificity. They are inhibited by a number of natural products, such as okadaic acid, cyclosporin A, and microcystin LR.[7,11] The only phosphatase inhibitors in current clinical use (as immunosuppressants) target PP2B.[12] PP2C, the archetypal member of the PPM family, is less well-characterized compared to the PPPs in terms of active site regulation.[10,13,14] The only known regulator of PP2C is divalent metal, typically Mg^{2+} or Mn^{2+} (Figure 1); no targeting subunits are known. Increasing evidence suggests that PP2Cs dephosphorylate T-loop-activated kinases of cell cycle checkpoints and stress-response pathways, including cyclin-dependent kinases (CDKs),[15,16] AMP-activated protein kinases (AMPKs),[17] and various mitogen-activated protein kinases (MAPKs) in the p38 and JNK pathways.[18,19] Other notable PP2C targets include autophosphorylated Ca^{2+}/calmodulin-dependent protein kinase II (CaMKII),[20] dopamine and cAMP-regulated phosphoprotein

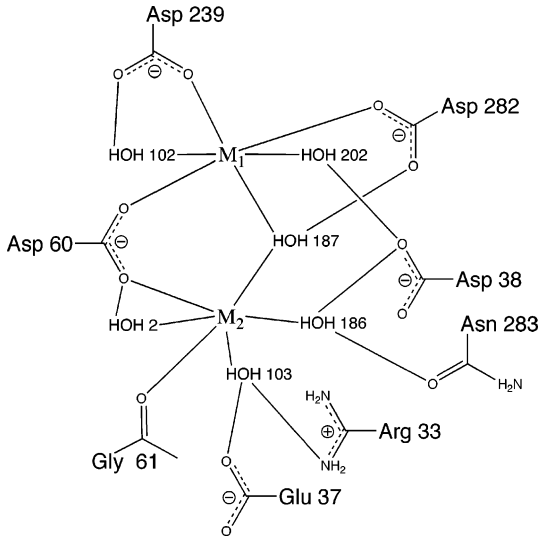

Figure 1. PP2Cα active site depicted as a two-dimensional projection based on the X-ray crystal structure (1A6Q). Residues are shown that make potential hydrogen bonding or electrostatic interactions to the active site metals or metal-coordinated waters.

* To whom correspondence should be addressed. For A.J.O.: phone, 858-784-9706; fax, 858-784-2980; e-mail, olson@scripps.edu. For P.G.: phone, 212-327-8780; fax, 212-327-7746; e-mail, greengard@rockefeller.edu.
† The Rockefeller University.
# These authors contributed equally to the work described in the paper.
‡ The Scripps Research Institute.
|| Current address: Department of Biochemistry and Biophysics, Arrhenius Laboratory, Stockholm University, SE-106 91 Stockholm, Sweden.
§ Current address: Department of Psychiatry, Yale University School of Medicine, New Haven, CT 06508.

10.1021/jm051033y CCC: $33.50
Published on Web 02/11/2006

of apparent M_r = 32000 (DARPP-32),[21] and metabotropic glutamate receptor subtype 3 (mGluR3).[22] The known inhibitors of the PPP Ser/Thr phosphatases do not affect PP2C activity;[7,11] no molecules analogous in effect or potency have been discovered for PP2Cs.

To identify inhibitors of PP2C, we applied a strategy that combined computational docking methods with a robust biochemical assay. The AutoDock molecular modeling program was used to conduct virtual ligand screening (VLS) with the National Cancer Institute (NCI) Diversity Set and the human PP2Cα crystal structure.[23] AutoDock is a suite of automated docking tools that predicts protein−ligand conformations and binding energies using an empirically calibrated force field, which is projected onto a regular grid for intermolecular energy calculations.[24−26] The method features full ligand flexibility and a relatively small estimated error of 2.177 kcal/mol in predicting binding free energies for docked ligands. The NCI Diversity Set, chosen as an initial database for lead compound identification, is 1990 compounds derived from around 140 000 compounds submitted to the NCI from a range of sources worldwide (http://dtp.nci.nih.gov/branches/dscb/diversity_explanation.html). In using this diverse subset of pharmacophores as a database, we were able to screen a wide range of chemical structures for binding to PP2C using less extensive computational resources than would be needed to screen a more typically sized database. In addition, compounds from the Diversity Set, as well as the larger (250 000+ structures) Open NCI Database, are available from the NCI for experimental testing. The Diversity Set compounds with experimentally demonstrated inhibitory activity were used as templates for similarity and chemical substructure searches in the Open NCI Database using the Enhanced NCI Database Browser, a Web-based graphical user interface with a large number of possible query types and output formats.[27] Those compounds were then ranked by AutoDock and assayed in the same way, in an efficient, iterative process.

Until now, few compounds have been described that can affect PP2C phosphatase activity, and the lack of specific inhibitors has strongly limited the identification of in vivo substrates. Here, we describe the use of virtual ligand screening for successful identification of several novel compounds that inhibit PP2Cα in the micromolar range. These reagents may be useful analytical tools, to elucidate the roles of this enzyme in intracellular signaling pathways, as well as leads for pharmaceuticals. Notably, this search strategy utilizes software and compounds that are freely available to academic researchers, and the search techniques described here should be generally feasible for any users interested in inhibitor discovery.

Results

Validation of AutoDock with PP2C for Virtual Ligand Screening. Initial docking calculations were performed using phosphoamino acid substrates as ligands to evaluate PP2C as a structural model for VLS. Phosphoserine (pSer), phosphothreonine (pThr), and *p*-nitrophenol phosphate (pNPP) were docked to the PP2Cα active site. AutoDock determined similar binding positions for all three compounds, with lowest predicted binding free energies of −7.45, −7.34, and −5.21 kcal/mol for pSer, pThr, and pNPP, respectively. The calculated locations of the phosphate groups of these compounds matched well with the location of a free phosphate molecule observed in the crystal structure[23] (Figure 2), which is proposed to represent the position of the actual substrate.

Identification of Lead Compounds Using AutoDock with the NCI Diversity Set. Following the success of the control dockings, VLS calculations were performed with the PP2Cα crystal structure model (containing metal and metal-coordinated waters) using a database of compound structures from the NCI Diversity Set. The VLS results were sorted on the basis of their predicted binding free energies, which ranged from −12.16 to +3.40 kcal/mol (Figure 3). Thirty percent of the energies were greater than the predicted energy of the pSer control. The top-ranked compounds from the VLS were chosen for further study.

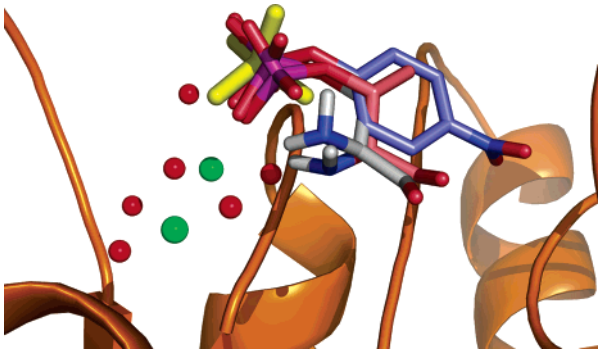

Figure 2. Control docking results. The lowest energy docked positions of pNPP (light blue), pSer (gray), and pThr (pink) are shown as stick representations surrounded by a ribbon model of PP2Cα (1A6Q). For the ligands, oxygen is red, nitrogen blue, and phosphorus purple. The crystallographic phosphate group is shown in yellow, and the positions of metal and water are indicated by green and red spheres, respectively.

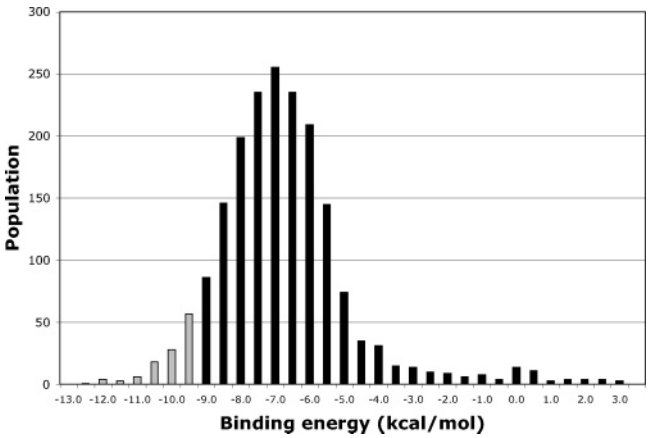

Figure 3. Results of AutoDock with NCI Diversity Set and PP2Cα. Bars represent numbers of Diversity Set compounds with predicted free energies of binding in the indicated 0.5 kcal/mol bins. Gray bars highlight the energies of the top-ranked 100 compounds.

Characterization of the Docking Site Based on VLS Results. Inspection of the docked positions of the top-ranked compounds revealed three distinct binding pockets close to the PP2C active site, termed sites I−III (Figure 4), with particular chemical group preferences. Nitrogen heterocycles and other nitrogen-rich groups were often found at site I. Site I is adjacent to the metal binding site and contains several aspartic acid residues (Asp 146, Asp 239, Asp 243, and Asp 282) capable of forming hydrogen bonds to amine hydrogens or stabilizing the heterocycles electrostatically. In addition, two aromatic ring binding sites (sites II and III) were identified. Site II is a central pocket formed by His 62, Leu 191, Ala 192, and Val 193. This site is the largest and most commonly occupied of the binding pockets, accommodating the largest rigid portion of a bound molecule. Site III is a narrow site comprising Arg 33, Val 34, Glu 35, Glu 37, and residues from the N-terminus, such as Gly 2 and Ala 3. The shape of this binding pocket complements

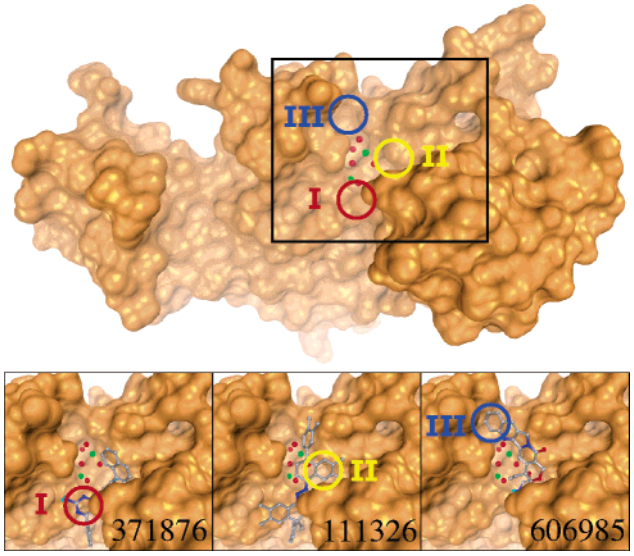

Figure 4. Binding pockets near the PP2C active site. Top panel shows a surface representation of the PP2Cα structure (1A6Q), with the active site area at the center of the box. Three binding pockets frequently occupied by particular chemical groups in the lowest energy docked structures of Diversity Set compounds are circled and labeled I, II, III. Lower panel shows top-ranked compounds whose docked positions typify binding at those sites.

relatively flat groups, such as phenyl rings, while the charged side chains that line the pocket complement polar and charged groups.

Discovery of PP2C Inhibitors Using ^{32}P-Based Phosphatase Assay. Assessment of the top-ranked compounds from the VLS as potential inhibitors of PP2C was performed using a standard radioactive assay, measuring PP2Cα dephosphorylation of ^{32}P-labeled mGluR3 substrate. Some compounds were sparingly soluble (either in the DMSO stock solution or in the reaction itself) and/or colored, but neither feature was prohibitive for this assay. The NSC numbers (National Service Center/NCI reference numbers), chemical structures, activities, and physical features of compounds exhibiting significant inhibitory activity (more than 30% inhibition) are listed in Table 1, along with the AutoDock binding energies.

The first set of compounds evaluated experimentally consisted of the top 100 compounds from the Diversity Set dockings, excluding those that were not available from the NCI and those with high calculated log *P* values (see Methods). Three compounds from this set, tested at 100 μM, inhibited more than 50% of PP2Cα activity: compounds 109268, 401366, and 402959 (Table 1). One additional compound, 12155, resulted in more than 30% inhibition (Table 1). The AutoDock VLS ranks of these inhibitors among the Diversity Set compounds were 3, 20, 35, and 87 for compounds 109268, 402959, 12155, and 401366, respectively.

Compounds 109268 and 401366, the most potent soluble inhibitors, were investigated further and were found to produce concentration-dependent inhibition of PP2Cα activity, with IC_{50} values in the 5−10 and 20−30 μM ranges, respectively. Simple control experiments were performed to test whether the observed inhibition was specific to the compound. For 109268, a copper-containing compound, the effect of Cu^{2+} was tested; an IC_{50} of 0.5−1 mM was determined for $CuCl_2$, and a negligible effect of millimolar concentrations of copper ligands such as L-His (a physiological ligand of copper ions) and imidazole on 109268 inhibition was demonstrated. Because 401366 and many of the top-ranked compounds were nitrogen-rich, several common chemicals with amino moieties were evaluated, and GuHCl, urea, spermidine, 6-aminocaproic acid, 1,6-diaminohexane, taurine, and L-Arg at 100 μM were determined to have no inhibitory effects on the phosphatase.

Docked Structures of Lead Diversity Set Inhibitors. The lowest energy docked structures of the first-generation inhibitors identified by the ^{32}P assay were analyzed in detail, in the context of sites I−III described above. Figure 5 (upper panel) illustrates the conformations of these four Diversity Set inhibitors at the docking site, and Figure 6 illustrates the specific PP2C side chain interactions of compounds 109268 and 401366.

Compound 109268 is a symmetric molecule with two 2-naphthol and piperidine-containing organic moieties bridged by two copper atoms and two chlorides. One piperidinyl component binds deeply within site III, with the corresponding naphthyl positioned within a shallow surface cavity beside Ala 63 and Gly 64 (see Figure 6 for details). The two central copper atoms and one of the 2-naphthol oxygens interact with the metal-bound waters. The second naphthyl group binds at site II, and the second piperidinyl group is directed toward the solvent rather than against the protein surface.

Compound 401366 is a phenanthryl compound with a nitrogen-rich tail at the 9-position. The phenanthryl rings fit into site II, forming a partial π-stacking interaction with the His 62 imidazole ring (see Figure 6 for details). The nitrogen-rich tail binds at site I and is also proximal to Lys 165.

Compound 402959 is composed of two 8-iodo-10-phenylphenazinyl groups connected by an amino linker. One phenyl ring is inserted into site III, with the corresponding phenazinyl group packed against the N-terminus. The linker amine interacts with metal-bound waters. The second phenyl binds in a pocket outside site I, between Arg 33 and Asp 239, while the second phenazinyl group lies in site I. The iodo components are not predicted to make significant electrostatic interactions with PP2C.

Compound 12155 is a urea compound containing two 4-amino-2-methylquinolinyl groups attached at the 6-position. One quinolinyl group inserts into site II, potentially forming a hydrogen bond between the 4-amino group and the Ser 190 carbonyl oxygen. The urea nitrogens form hydrogen bonds in site I to Asp 239 and metal-bound waters and are also electrostatically stabilized by Asp 146 and Asp 282. The second quinolinyl group rests in a pocket outside site I and forms hydrogen bonds between the 4-amino group and Ser 190 and Asp 243.

Refinement of Lead Inhibitors. Second-generation lead compounds were identified by docking and assaying compounds from similarity searches, based on chemical structures and substructures of the Diversity Set leads. Around 6000 compounds were identified from the similarity searches and docked, and 2.6% of those, selected from the highest-scoring in various searches, were evaluated using the ^{32}P-based assay. Compounds related by Tanimoto similarity to primary leads 109268 (109272) and 402959 (5020) were, like their prototypes, found to have IC_{50} values less than 100 μM (Table 1). Inhibition was observed as well for compounds comprising chemical groups suggested by the Diversity Set dockings, including triazinanes, related to the nitrogen-rich portion of primary lead 401366 (5206, 127153, and 128184), and naphthyls (345647) (Table 1).

Several representative inhibitors from both the first- and second-generation screens were tested for nonspecific, aggregation-based inhibition, characterized by significant sensitivity to detergent and enzyme concentration.[28] PP2C inhibition by compounds 5020 and 5206 was decreased considerably (by an

Table 1. Activities, AutoDock Binding Energies, and Physical Properties of PP2C Inhibitor Compounds

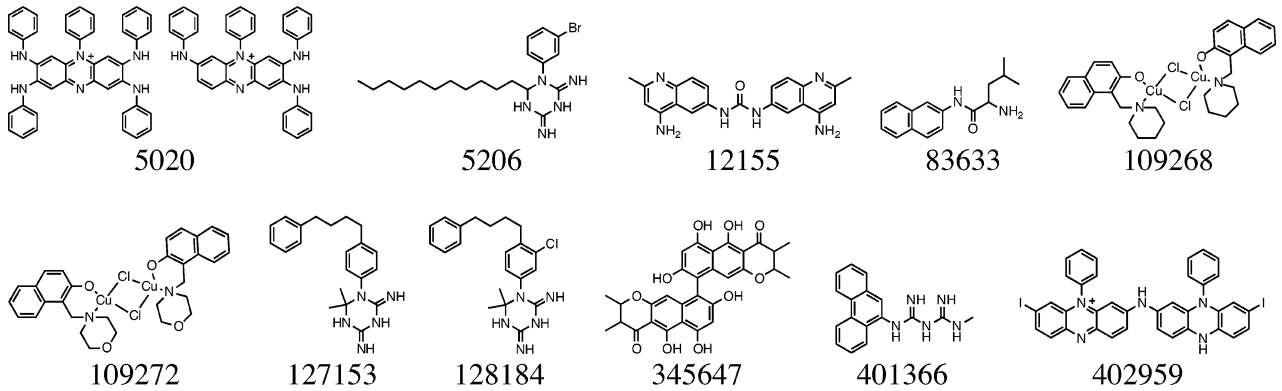

NSC no.	fraction PP2C activity[a]	AutoDock binding energy (kcal/mol)[b]	color/solubility/ aggregates[c]	molecular weight	no. H-bond acceptors	no. H-bond donors	no. rotatable bonds
5020	0.04	−8.61, −9.97	+ • ∇ #	622, 530	5, 4	4, 3	9, 7
5206	0.06	−9.49	#	459	5	4	11
12155	0.61	−9.98		372	6	4	3
83633	0.64	−8.68		256	2	2	4
109268	0.18	−11.79	+ •	679	2	2	0
109272	0.22	−13.61	+ •	684	4	2	0
127153	0.51	−9.89		349	5	4	6
128184	0.54	−10.06		384	5	4	6
345647	0.38	−10.01	+	547	10	6	1
401366	0.35	−9.24		328	5	5	5
402959	0.32	−10.33	+ • ∇	780	4	2	4

[a] Fraction PP2C activity with compound present at 100 μM. [b] For compound 5020, fraction activity refers to the 1:1 mixture. Other parameters are given separately, with the larger component first. For compound 83633, the energy is given for the original VLS. This compound was identified as an inhibitor based on docking to the apo model, where the energy was −12.91 kcal/mol. [c] Symbols indicate physical properties as follows: +, 10 mM DMSO stock solution is colored; •, limited or unclear solubility in stock solution; ∇, precipitation upon dilution in phosphatase reaction; #, possible formation of aggregate particles.

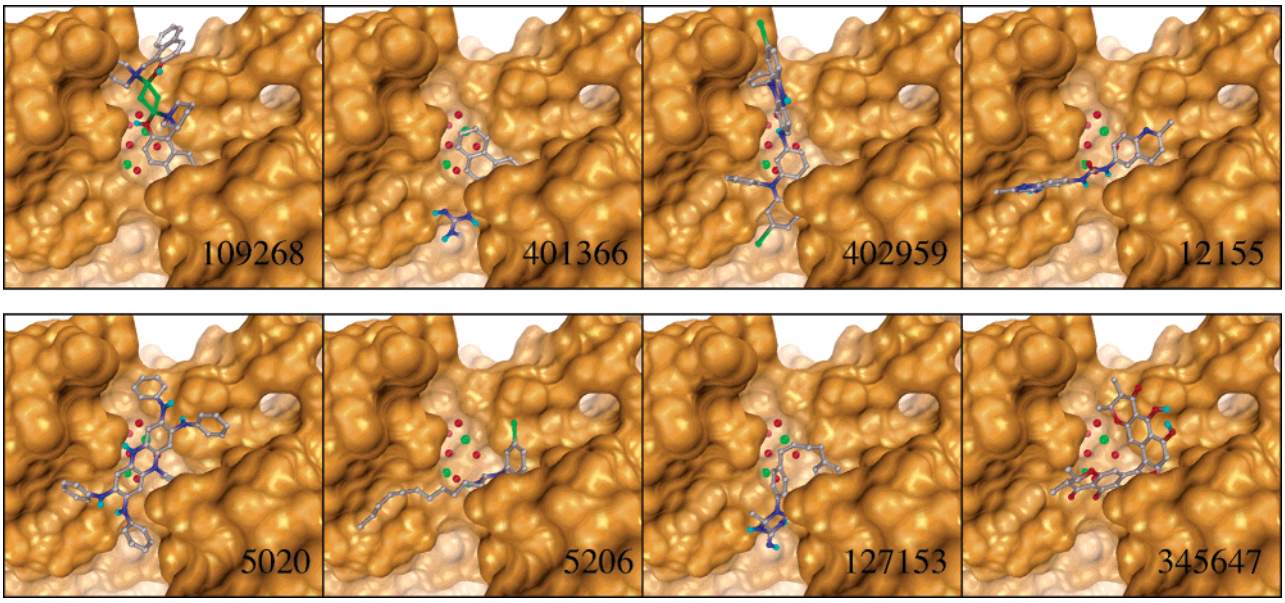

Figure 5. Predicted binding positions of PP2C inhibitors. Upper panel shows compounds discovered from the NCI Diversity Set. Lower panel shows compounds from the second round of screening, with compounds from the Open NCI Database.

order of magnitude) in the presence of nonionic detergent and upon a 10× increase in enzyme concentration. However, inhibition by compounds 12155, 109268, 109272, 128184, 345647, 401366, and 402959 under those conditions varied only by 1- to 3-fold, compared to inhibition under the standard conditions.

Docked Structures of Second-Generation Inhibitors. The lowest energy docked structures of four representative second-generation inhibitors are shown in Figure 5 (lower panel). The predicted binding position of 109272 (not shown) is very similar to that of 109268 (Figure 5, upper panel), with some small variations in the orientations of the ring structures.

Compound 5020, an induline dye, is a 1:1 mixture of tetraphenyltriamine and pentaphenyltetramine phenazines (Table 1). The two molecules, docked separately, showed similar lowest energy conformations; the larger, N^2,N^3,N^7,N^8-5-pentaphenyl-5λ^5-phenazine-2,3,7,8-tetramine, is shown. A hydrogen bond is formed between Arg 33 and the nitrogen at the central 10-position in the heterocycle. The other, phenyl-bearing heterocycle nitrogen at the 5-position may interact with the metal-

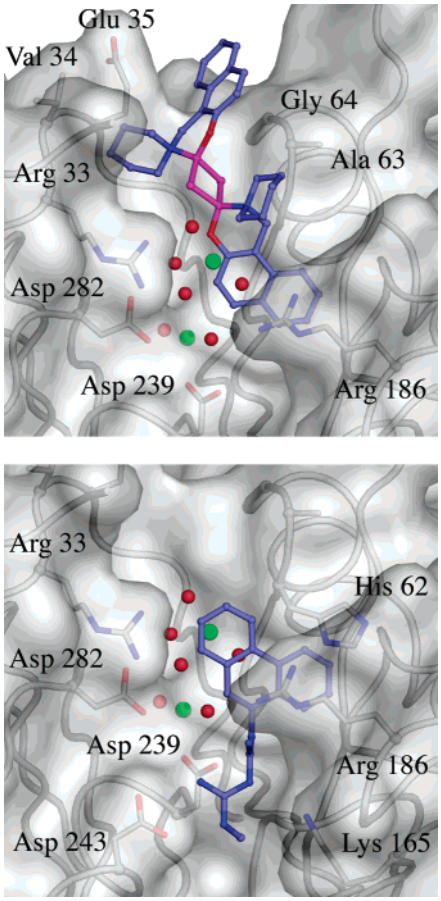

Figure 6. Predicted interactions of compounds 109268 (top) and 401366 (bottom) with residues near the PP2C docking site. Oxygen is red, nitrogen blue, and copper magenta. Positions of metal and water are indicated by green and red spheres, respectively.

bound water molecules via its electron pair. The N^8-phenyl group (not found in the smaller molecule) binds in a pocket between Asp 243 and Asp 282, neighboring site I. The N^7-amide proton potentially hydrogen-bonds with Asp 146 and Asp 239. The N^7-phenyl fits into site I, the 5-phenyl fits into site II, and the N^2-phenyl fits into site III. The N^3-phenyl fits into a surface cavity neighboring site II and interacts with residues Asp 199, His 62, and Ala 63.

Compound 5206 contains a 1,3,5-triazinane-2,4-diimine core, which binds at site II and forms hydrogen bonds to Asp 146 and Asp 239. The bromophenyl group attached to the nitrogen heterocycle binds in a neighboring surface groove formed by residues His 62, Arg 186, and Leu 191. The 11-carbon acyl tail binds in an elongated surface cavity formed between Ser 280 and Asp 243 and Asp 282.

Compound 127153 contains a 1,3,5-triazinane-2,4-diimine core, which binds at site I and forms hydrogen bonds to Lys 165, Asp 146, Asp 239, and Asp 243. The phenyl ring nearest the nitrogen heterocycle is positioned between Arg 33 and Arg 186 and neighbors the metal-bound waters. The butyl chain within the binding site positions the second phenyl ring at site II. Compound 128184 has the same structure as 127153 but with a chlorine at the 3-position of the first phenyl ring. This compound (not shown) is predicted to bind very similarly to 127153, with the additional chloride positioned near the active site metals.

Compound 345647, a chaetochromin, comprises a core of two naphthopyrandione groups connected at the 9-position. One naphthopyran group binds partially at site I, forming hydrogen

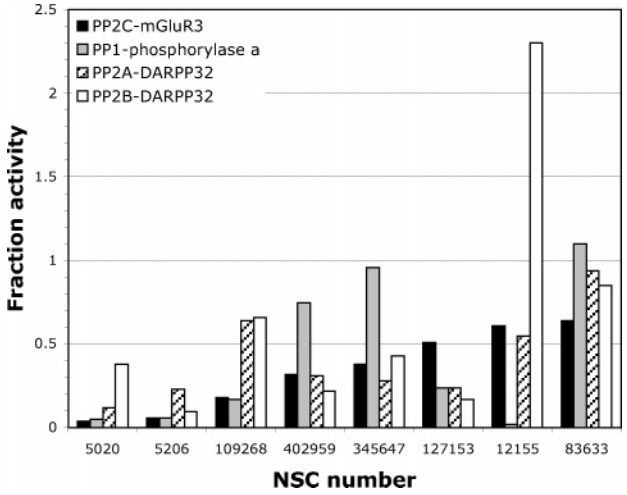

Figure 7. Effects of selected PP2C inhibitors on PPP phosphatases. Bars represent the fraction of total phosphatase activity present when compounds were added at 100 μM. A fraction of 1.0 indicates no inhibition of enzyme, whereas a fraction of 0.5 indicates an IC_{50} of around 100 μM. Activity of PP2C is indicated in black, PP1 in gray, PP2A in diagonal stripe, and PP2B in white. Compounds are listed from left to right in order of increasing residual PP2C activity or decreasing PP2C inhibition.

bonds with Asp 146 and Asp 239 as well as a metal-bound water, and spans the docking site to fit into site II. The second naphthopyran group binds in a pocket adjacent to site II, shaped by Leu 191 and Val 193, forming a hydrogen bond between a hydroxyl proton and the Leu 191 carbonyl. This second group also spans the docking site, to bind at site III.

Evaluation of Docking Model. In parallel with the in vitro inhibitor identification, several different approaches were taken to assess basic features of the structural model used to dock. On the basis of the first Diversity Set leads, dockings of 109268 and 401366 were performed using all possible models for the six bound water positions. For compound 109268, model 001111 (see Methods for binary code) was the best and model 011000 the worst; for compound 401366, model 000011 was the best and model 010000 the worst. The differences in AutoDock binding energies between the best and worst water models were 2.41 and 2.95 kcal/mol for compounds 109268 and 401366, respectively. Differences between the best and full water models were 1.89 and 1.78 kcal/mol. In addition, the entire Diversity Set was docked to models lacking the binuclear metal center (metal and associated waters, termed apo) or lacking the six waters (waterless). The apo model dockings resulted in binding energies ranging from −19.59 to +0.56 kcal/mol; the analogous range was −12.41 to +0.56 kcal/mol for the waterless model dockings. Overlap with the original Diversity Set VLS between the top 100 compounds was 31% for the apo docking model and 42% for waterless. Assay of the top 40 compounds from the apo model dockings that were not redundant with previously tested molecules identified compound 83633, which at 100 μM inhibited more than 30% of PP2Cα activity (Table 1).

Activity of PP2C Inhibitors at PPPs. Figure 7 illustrates the effects of eight of the PP2C inhibitors identified here on three additional mammalian Ser/Thr phosphatases, the prototypical PPPs PP1, PP2A, and PP2B. Compounds 5020 and 5206 inhibited PP2C and all the PPPs tested, with inhibition decreased for 5020 at PP2B and for 5206 at PP2A. Compound 109268 inhibited PP1 at a level similar to that of PP2C, with inhibition significantly decreased at PP2A and PP2B. Compounds 402959 and 345647 inhibited PP2A and PP2B at a level similar to that of PP2C but showed little inhibition at PP1. Compound 127153

was a better inhibitor of all the PPPs tested compared to PP2C, with an IC_{50} of ~50 μM at PP1, PP2A, and PP2B: approximately half its IC_{50} value at PP2C. Compound 12155, a moderate inhibitor of PP2C and PP2A, at 100 μM inhibited nearly all PP1 activity and increased PP2B activity over 3-fold. Compound 83633, a moderate inhibitor of PP2C identified in the apo model dockings, had little effect on the activity of any of the PPPs tested.

Discussion

PP2C Docking Model. Certain features of the PP2Cα crystal structure complicated its use as a docking model. The bi-Mn^{2+} active site of PP2Cα, which directly coordinates six water molecules, presented several possible models for docking, as any of the waters or metals could potentially be displaced upon inhibitor binding. Additionally, the PP2Cα crystal structure was determined with phosphate ion from the crystallization buffer bound at the active site; it is not known if the protein conformation changes substantially upon substrate or inhibitor binding. Because of differences between free and ligand-bound forms of a protein, structures without substrate or inhibitor bound are often less successful for docking studies than ligand-bound structures.[29] Nonetheless, the crystallographic phosphate position provided valuable information for molecular modeling. Since the phosphate ion binds and most likely forms hydrogen bonds with four waters coordinating the active site metal cofactors, it has been proposed that its position represents the binding site for the phosphorylated substrate.[23] The docking results for the phosphoamino acids support this idea as all three amino acid phosphates find optimal binding positions within 1 Å of the free phosphate position. These results suggest that the structural model of PP2Cα together with metal ions and full water coordination can be successful for docking calculations.

Docking results for the Diversity Set with apo or waterless models of PP2C were not drastically different compared to the results using the original structural model. However, docking with individual inhibitors and different water models revealed a distinct preference for deletion of water 102. Among the highest-ranked models, there was also a suggested preference of compound 109268 for the presence of water 187 (consensus x0xx1x, where x denotes no preference) and of compound 401366 for deletion of water 2 (00xxxx). These observed preferences are potentially meaningful given that the catalytic mechanism used by PP2C, unlike those of protein tyrosine and alkaline phosphatases, is proposed to involve direct phosphoryl transfer to water, with no phosphoenzyme intermediate.[10] For PP2C, water molecules also play a critical role in coordinating metal ions, which have been proposed as pseudosubstrates and bind the enzyme prior to the phosphorylated moiety.[30] Water 187 bridges the two metal ions (Figure 1) and may act as the catalytic nucleophile.[23] Waters 2 and 102 bridge metal ions and PP2Cα residues Asp 60 and Asp 239, respectively; mutation of either of these two residues to Asn was found to increase the K_{metal} value of PP2Cα by 1 order of magnitude while decreasing the k_{cat} by 3 orders.[31]

PP2C Inhibitors and Potential Pharmacophores. Using VLS in combination with an in vitro phosphatase assay, we have found molecules that inhibit PP2C dephosphorylation of a physiological substrate. In the past, only high, millimolar concentrations of phosphate analogues such as pyrophosphate and orthovanadate, or divalent cations such as Ca^{2+} were known to inhibit PP2C. Here, we have identified compounds with several different organic scaffolds that inhibit PP2C in a concentration-dependent manner at low micromolar concentrations. Physical properties of these compounds (Table 1) are druglike, in terms of the rule of five[32] or the combination of rotatable bonds and polar surface area.[33] Most importantly, in the structures of these lead compounds certain core elements are suggested, which might be investigated further as the foundation for more potent, more specific PP2C inhibitors and/or therapeutics.

One example of such a potential core is the nitrogen-rich tail of compound 401366. Expressed in cyclic form, this tail is a 1,3,5-triazinane-2,4-diimine, and our second-generation screening (docking and assay of compounds incorporating triazinane and imine) showed that several of these triazinanes were also PP2C inhibitors. In the lowest energy docked conformations, the linear and cyclic forms of the nitrogen-rich string, found in compounds 401366 and 127153/128184, respectively (but not 5206), are positioned similarly at the active site (Figure 5). For this particular core, a certain amount of negative data was amassed, which began to implicate specific elements critical to PP2C inhibition by these compounds. For example, compounds very similar to the 401366 lead (14743 and 14747) and its constituents (26256 and 91485) were found to have no effect on PP2Cα activity. The *N*-methyl terminus of the dicarbonimidodiamide tail of compound 401366 may be especially important for inhibition. An analogous result was found with compounds 5206 and 3082, which differ only in the substituent (undecyl versus dimethyl) at the 6-position. The 1,3,5-triazinane-2,4-diimine core (specifically, derivatized with extended hydrophobic chains at position 1 or 6) or a similar string is a distinct inhibitor scaffold to explore.

Another strong component of PP2C inhibitors highlighted by these lead compounds is ring systems, particularly of two (naphthalene, quinoline) or three (phenanthrene, phenazine) rings, often including amino groups. The importance of fused-ring components was also indicated in two recent studies testing simple analogues of phosphonothioic and phosphonic acids as nonhydrolyzable phosphate ester mimics, in which a carboxynaphthyl moiety was found to confer notable inhibition of PP2C.[34,35] On the basis of the docking conformations of the leads identified here, the combination of a fused-ring group (for which there appear to exist complementary binding pockets adjacent to the active site) with a group bound near where the substrate would bind (specifically, near Arg 33, which is known to affect the K_m for the pNPP substrate,[31] and metal-bound water 102) may be a promising general formula for a PP2C inhibitor.

Lead Compound Activity at Other Ser/Thr Phosphatases. Although known PPP inhibitors do not inhibit PP2C, these NCI compounds identified as PP2C inhibitors are, conversely, generally active at PPPs. Immediately, questions arise as to what particular features of these compounds make them accessible to PP2C as well as other Ser/Thr phosphatases. It is striking, moreover, that these compounds do not follow the common pattern of PPP inhibition, in which many natural product inhibitors are potent inhibitors of PP1 and PP2A (often, as with okadaic acid, favoring PP2A), showing lower but relatively potent (low micromolar) inhibition of PP2B.[7,36] Rather, these PP2C inhibitors discriminate between closely related Ser/Thr phosphatases in novel ways.

Few small molecules that are specific for different PPPs are known or have been designed, despite a number of structure−activity relationship (SAR) studies.[7] The antitumor compound fostriecin (aka CI-920), a soluble phosphate monoester discovered in a subspecies of *Streptomyces*, is the most selective PPP inhibitor known, with a 10^4 preference for PP2A (IC_{50} = 3 nM) versus PP1.[37] Selective leads for the other PPPs include

tautomycetin for PP1 (IC_{50} = 2 nM; PP1/PP2A selectivity of ~30-fold)[38] and an endothall derivative incorporating a *trans*-cyclopropylphenyl group for PP2B (apparent K_i = 0.5 μM; PP2B/PP1 selectivity of 8-fold).[39]

Among our leads, the compound showing the greatest selectivity for a single Ser/Thr phosphatase is compound 12155 for PP1. Compound 12155 is further distinguished by its strong activation of PP2B; some activating effects were seen with other compounds tested at PP2C but not at this high level of activation. Other interesting selectivities include compound 109268 for PP1 and PP2C versus PP2A and PP2B and compound 127153 for PPPs in general versus PP2C. Compounds 345647 and 402959 are also distinguished by significantly poorer inhibition of PP1, compared to PP2C, PP2A, and PP2B. Overall these PP2C inhibitors are not as potent or selective as those best examples mentioned above. They are important though in that they represent fresh models for SAR studies, to begin to formulate a more general understanding of selective PPP and PPP/PPM inhibition.

Functional Connections from NCI Database Leads. As the Diversity Set and Open NCI Database are used increasingly, it will be possible to find a growing amount of existing information on any compound identified in a new study. Coordination of information from various studies associating lead compounds with particular activities can reinforce and expand the understanding of acknowledged roles of target proteins, and perhaps evoke new ones.

An example of the former case for PP2C involves inhibitors identified here that have been found in other screens in association with cell-cycle regulation. In a yeast screen performed by the NCI,[40] compounds 5206, 12155, 109268, and 345647 were found to inhibit growth of yeast strains with alterations in DNA damage repair or cell cycle control (http://dtp.nci.nih.gov/docs/dtp_search.html). Another screen, using high-content flow cytometry to search for compounds that enhanced the antilymphoma activity of rituximab (a monoclonal antibody in current clinical use), identified compound 12155.[41] PP2C has been implicated in these cancer-related areas previously (see also Introduction), supporting its connection to these results. Overexpression of PP2Cs has been known for some time to inhibit DNA synthesis and cause cell cycle arrest.[42,43] In addition, PP2Cs have been shown to bind and dephosphorylate kinases involved in DNA damage and replication checkpoint pathways, such as homologues of Chk1[44,45] and Chk2,[46] and a glycosylase involved in DNA damage repair.[47] Recent evidence suggests that one PP2C subtype, termed Wip1 or PPM1D, may be an important tumor promoter as Ppm1d-null mice were found to be resistant to mammary tumors induced by Hras or Erbb2.[48] This tumorigenic function makes Wip1,[49,50] and conceivably other PP2Cs, especially desirable targets for a small-molecule inhibitor drug.

The PP2C inhibitor leads reported here have also been associated with other activities in which PP2C has not been known to be involved. For example, several Diversity Set screens have identified certain of our lead compounds as protease inhibitors. Compound 109268 and analogues such as DCPTC [dichloro(1,10-phenanthroline)copper(II)] and 8+C (1:1 complex of 8-hydroxyquinoline hemisulfate and $CuCl_2$) were recently identified as proteasome inhibitors, decreasing the chymotrypsin-like activity and inducing apoptosis in human leukemia and prostate cancer cells.[51] Compound 12155 was found, using a combination of fluorescence and HPLC-based assays, to inhibit anthrax toxin lethal factor, a zinc-dependent protease that targets proteins in the MAPK kinase family.[52] Screening for inhibition of another zinc-dependent protease, botulinum neurotoxin type A light chain, identified compound 402959.[53] The connection between proteases and PP2C through these common inhibitor molecules may be meaningful, reflecting similarity in active sites and/or physiological cross-reactivity not previously considered. Studies using the NCI databases for targets other than PP2C may converge to suggest interesting new functional connections as well.

Conclusion

We have applied virtual ligand screening of compounds from the NCI database to identify micromolar inhibitors of PP2C, a Ser/Thr phosphatase of the PPM family. These results compare well with micromolar results achieved with VLS studies of other enzymes employing different software packages[54−57] and with other compound screening studies that have used the NCI Diversity Set[58] (see also Discussion). The molecules described here are the only non-phosphate-based compounds known to inhibit PP2C, and suggest elements and factors that will be important for the development of PP2C inhibitor design strategies and applications. We are currently pursuing protein crystallography studies to visualize the PP2C−inhibitor complexes. Future investigations based on the inhibitor molecules identified here will lend needed insight into the mechanism, targeting, and therapeutic potential of this phosphatase.

Methods

AutoDock Identification of Lead Compounds. The AutoDock 3.0 software package,[26] as implemented through the graphical user interface called AutoDockTools (ADT), was used to dock small molecules to PP2Cα. The enzyme file was prepared using published coordinates (PDB 1A6Q). The two metal atoms and six metal-coordinating water molecules within the putative active site were retained with the protein structure. The metal atoms were each manually assigned a charge of +2 and a solvation value of −30. The terminal residues were modified to charged quaternary amine and carboxylate forms, and residues 321 and 326, which formed the ends of a gap in the crystal structure, were given standard residue charges. All other atom values were generated automatically by ADT. The docking area was assigned visually around the presumed active site. A grid of 30 Å × 30 Å × 30 Å with 0.375 Å spacing was calculated around the docking area for 13 ligand atom types using AutoGrid. These atom types were sufficient to describe all atoms in the NCI database. For model validation, the structures of pSer, pThr, and pNPP were generated using Insight II (Accelrys) and converted to AutoDock format files using ADT. For VLS, compound structures (http://dtp.nci.nih.gov/docs/3d_database/structural_information/structural_data.html) from the NCI Diversity Set were prepared for use with AutoDock. PDB files excluded from docking calculations were those with atom types not readily assigned a partial charge and those with incorrect geometries not remedied by changes in rotatable bonds. Transition metals were given neutral charge. An AutoDock-ready database of the NCI Diversity Set is available at http://www.scripps.edu/mb/olson/dock/autodock/.

For each ligand, eight separate docking calculations were performed. Each docking calculation consisted of 25 million energy evaluations using the Lamarckian genetic algorithm local search (GALS) method.[26] The GALS method evaluates a population of possible docking solutions and propagates the most successful individuals from each generation into the subsequent generation of possible solutions. A low-frequency local search according to the method of Solis and Wets is applied to docking trials to ensure that the final solution represents a local minimum. All dockings described in this paper were performed with a population size of 200, and 300 rounds of Solis and Wets local search were applied with a probability of 0.06. A mutation rate of 0.02 and a crossover rate of 0.8 were used to generate new docking trials for subsequent

generations, and the best individual from each generation was propagated to the next generation. The docking results from each of the eight calculations were clustered on the basis of root-mean-square deviation (rmsd) between the Cartesian coordinates of the atoms and were ranked on the basis of free energy of binding. The top-ranked compounds were visually inspected for good chemical geometry.

Preparation of NCI Compounds. Compounds determined by AutoDock to have low binding energies to PP2Cα were requested in groups of 40 and received from the Drug Synthesis and Chemistry Branch, Developmental Therapeutics Program, Division of Cancer Treatment and Diagnosis, National Cancer Insititute (http://dtp.nci.nih.gov/branches/dscb/repo_request.html). The vialed solids were dissolved in DMSO to 10 mM stock concentrations and stored at room temperature. After the first group of 40 was tested, a log *P* filter was established. The octanol/water partition coefficients of the compounds were predicted using the program XLOGP;[59] compounds with log *P* values above 6.0 were not requested.

Preparation of Assay Components. PP2Cα (rat sequence, Swiss-Prot accession number P20650) was cloned in the pET23 vector (Novagen) using the NdeI and XhoI restriction sites, expressed in *E. coli* with a C-terminal 6-His tag, and batch-purified using Ni-NTA resin (Qiagen). The phosphatase was concentrated and stored in a buffer of 10 mM Tris, pH 7.5, 50 mM NaCl, 1 mM $MgCl_2$, and 2 mM DTT. The C-terminal tail of mGluR3 (residues 830−879) in the pGEX-4T-1 vector (Amersham Biosciences) was expressed in *E. coli* as a fusion to the C-terminus of GST and purified in batch format using glutathione sepharose 4B (Amersham Biosciences).[22] Concentration was estimated using a Coomassie-stained polyacrylamide gel and Benchmark protein standard (Invitrogen). The fusion protein bound to sepharose beads (≥10 μM) was phosphorylated using the catalytic subunit of PKA and 10 μCi/μL γ-^{32}P-ATP (Perkin-Elmer) followed by 200 μM unlabeled ATP (Sigma), in a buffer of 50 mM HEPES, pH 7.5, 10 mM $MgCl_2$, and 1 mM EGTA.

Assay for PP2C Inhibition. Phosphatase reactions were set up in 100 μL volumes, in a reaction buffer of 50 mM Tris, pH 8.0, 40 mM $MgCl_2$, 150 mM NaCl, 100 μg/mL BSA, and 5 mM DTT. Enzyme was diluted in reaction buffer as appropriate to give 20−30% final dephosphorylation, and reactions in triplicate were started by addition of ^{32}P-labeled mGluR3 slurry (typically 5 μM; 100000−200000 cpm), incubated with rotation for 30 min at room temperature, and stopped with 200 μL of 10% w/v trichloroacetic acid (TCA). Reaction mixtures were centrifuged, 200 μL of supernatant was removed to a separate tube, and the amounts of ^{32}P in both supernatant and precipitate were determined using Cerenkov counting. The effects of the NCI compounds on PP2Cα dephosphorylation of mGluR3 were determined by the fraction of enzyme activity remaining in reaction mixtures containing 100 μM compound; that is, the amount of dephosphorylation (cpm supernatant/cpm total, corrected for free ^{32}P in absence of enzyme) with compound divided by the amount of dephosphorylation without compound. To test for aggregation-based inhibition, the effects of identified inhibitors were tested under two additional conditions, 1 mg/mL saponin or 10 times the amount of enzyme used for the standard assay, and compared by ratio to the original values.[28]

Second-Generation Compound Screening. Lead compound structures identified by the combination of docking and activity assay were used to conduct similarity searches among more than 250 000 structures found in the Open NCI Database. The Enhanced NCI Database Browser[27] was used to search on the basis of substructure (by chemical name or SMILES (http://daylight.com) string) and/or similarity by Tanimoto coefficient,[60] with a cutoff of 0.85.[61] From these searches, selected compound structures were output to mol2 format files, prepared using ADT, and docked to PP2Cα using the same methods as for the Diversity Set. Compounds with the lowest predicted binding energies were requested and assayed for effect on phosphatase activity as described above.

Docking Model Modifications. Several variations on the protein model used to dock were evaluated as well. Compounds 109268 and 401366 were each docked using coordinates in which the six bound water molecules (included in the original dockings) were systematically deleted, generating all 64 possible water models. Models are denoted here by binary code, with 0 or 1 for the absence or presence of waters 2, 102, 103, 186, 187, and 202 (e.g., in model 011100, waters 2, 187 and 202 are deleted and 102, 103, and 186 are present). In addition, the entire Diversity Set was docked using two alternative protein models, one containing no water (waterless) and one containing no water and no metal (apo).

Assay for PPP Phosphatase Inhibition. Representative compounds identified as PP2C inhibitors were tested with three different phosphatases from the PPP family. The phosphatase−substrate pairs tested were PP1−phosphorylase *a*, PP2A−DARPP-32 pThr34 (DARPP-32 phosphorylated at Thr 34), and PP2B−DARPP-32 pThr34. PP1 catalytic fragment was purchased (Upstate); PP2A trimer and PP2B were partially purified from frozen rat brain. Phosphorylase *a* was prepared by published methods,[62] using phosphorylase *b* (Calzyme) and phosphorylase kinase (Sigma) from rabbit muscle with γ-^{32}P-ATP (Perkin-Elmer) in a buffer containing 100 mM Tris, pH 8.2, 100 mM sodium glycerol-1-phosphate, 0.1 mM $CaCl_2$, 10 mM magnesium acetate, and 0.2 mM ATP. The phosphorylation reaction was stopped on a PD-10 desalting column (Amersham Pharmacia), and phosphorylase *a* was precipitated at 45% saturated ammonium sulfate, resuspended in a buffer containing 50 mM Tris, pH 7.0, 0.1 mM EGTA, 10% glycerol, and 1 mM DTT, applied to a NICK desalting column (Amersham Pharmacia), and eluted in the same resuspension buffer. DARPP-32 pThr34 was prepared using rat DARPP-32 expressed in *E. coli* as a 6-His tag fusion, purified using a HiTrap chelating HP column (Amersham Pharmacia), and phosphorylated using PKA as described above for the GST−mGluR3 fusion, with separation from labeled ATP via a NICK column. PPP phosphatase reactions were typically set up in 30 μL volumes in a buffer of 50 mM Tris, pH 7.0, 0.1 mM EGTA 100 μg/mL BSA, 0.01% v/v Brij-35, 5 mM caffeine, and 1 mM DTT for PP1; the PP2C reaction buffer (see above) for PP2A; or a buffer of 20 mM Tris, pH 7.0, 100 mM KCl, 5 mM $CaCl_2$, 6 μg/mL CaM, and 1 mM DTT for PP2B. Reactions in duplicate were started with addition of ^{32}P-labeled substrate, incubated at room temperature for 10 min, and stopped with 100 μL of 10% w/v TCA. Tubes were vortexed and centrifuged for 2 min, and 100 μL of supernatant was removed to a separate tube. The amounts of ^{32}P in both supernatant and precipitate were determined using Cerenkov counting, with controls as described for the PP2C−mGluR3 reactions.

Acknowledgment. We thank Atsuko Horiuchi for providing PKA, and Heidi Erlandsen for reading the manuscript. This work was funded by Postdoctoral Grant T32 MH15125-25 from the National Institutes of Health (J.P.R.) and Postdoctoral Grant PF-02-087-01 from the American Cancer Society (A.E.B.); USAMRAA/DOD Grant DAMD17-02-1-0705, U.S. Public Health Service Grants MH40899, MH74866, and DA10044 (P.G. and A.C.N.), and the Michael Stern Parkinson's Research Foundation (P.G.); and Grant CA95830 from the National Cancer Institute (A.J.O).

References

(1) Cohen, P. The origins of protein phosphorylation. *Nat. Cell Biol.* **2002**, *4*, E127−E130.
(2) Hunter, T. Protein kinases and phosphatases: the yin and yang of protein phosphorylation and signaling. *Cell* **1995**, *80*, 225−236.
(3) Cohen, P. The role of protein phosphorylation in human health and disease. The Sir Hans Krebs Medal Lecture. *Eur. J. Biochem.* **2001**, *268*, 5001−5010.
(4) Manning, G.; Whyte, D. B.; Martinez, R.; Hunter, T.; Sudarsanam, S. The protein kinase complement of the human genome. *Science* **2002**, *298*, 1912−1934.
(5) Cohen, P. Protein kinases—the major drug targets of the twenty-first century? *Nat. Rev. Drug Discovery* **2002**, *1*, 309−315.
(6) Zhang, Z. Y. Protein tyrosine phosphatases: structure and function, substrate specificity, and inhibitor development. *Annu. Rev. Pharmacol. Toxicol.* **2002**, *42*, 209−234.

(7) McCluskey, A.; Sim, A. T.; Sakoff, J. A. Serine-threonine protein phosphatase inhibitors: development of potential therapeutic strategies. *J. Med. Chem.* **2002**, *45*, 1151−1175.
(8) Hunter, T. Signaling−2000 and beyond. *Cell* **2000**, *100*, 113−127.
(9) Cohen, P. The structure and regulation of protein phosphatases. *Annu. Rev. Biochem.* **1989**, *58*, 453−508.
(10) Jackson, M. D.; Denu, J. M. Molecular reactions of protein phosphatases. Insights from structure and chemistry. *Chem. Rev.* **2001**, *101*, 2313−2340.
(11) Sheppeck, J. E., 2nd; Gauss, C. M.; Chamberlin, A. R. Inhibition of the Ser-Thr phosphatases PP1 and PP2A by naturally occurring toxins. *Bioorg. Med. Chem.* **1997**, *5*, 1739−1750.
(12) Liu, J.; Farmer, J. D., Jr.; Lane, W. S.; Friedman, J.; Weissman, I.; et al. Calcineurin is a common target of cyclophilin-cyclosporin A and FKBP-FK506 complexes. *Cell* **1991**, *66*, 807−815.
(13) Barford, D.; Das, A. K.; Egloff, M. P. The structure and mechanism of protein phosphatases: insights into catalysis and regulation. *Annu. Rev. Biophys. Biomol. Struct.* **1998**, *27*, 133−164.
(14) Schweighofer, A.; Hirt, H.; Meskiene, I. Plant PP2C phosphatases: emerging functions in stress signaling. *Trends Plant Sci.* **2004**, *9*, 236−243.
(15) Cheng, A.; Kaldis, P.; Solomon, M. J. Dephosphorylation of human cyclin-dependent kinases by protein phosphatase type 2C alpha and beta 2 isoforms. *J. Biol. Chem.* **2000**, *275*, 34744−34749.
(16) De Smedt, V.; Poulhe, R.; Cayla, X.; Dessauge, F.; Karaiskou, A.; et al. Thr-161 phosphorylation of monomeric Cdc2. Regulation by protein phosphatase 2C in Xenopus oocytes. *J. Biol. Chem.* **2002**, *277*, 28592−28600.
(17) Davies, S. P.; Helps, N. R.; Cohen, P. T.; Hardie, D. G. 5′-AMP inhibits dephosphorylation, as well as promoting phosphorylation, of the AMP-activated protein kinase. Studies using bacterially expressed human protein phosphatase-2C alpha and native bovine protein phosphatase-2AC. *FEBS Lett.* **1995**, *377*, 421−425.
(18) Takekawa, M.; Maeda, T.; Saito, H. Protein phosphatase 2Calpha inhibits the human stress-responsive p38 and JNK MAPK pathways. *EMBO J.* **1998**, *17*, 4744−4752.
(19) Hanada, M.; Ninomiya-Tsuji, J.; Komaki, K.; Ohnishi, M.; Katsura, K.; et al. Regulation of the TAK1 signaling pathway by protein phosphatase 2C. *J. Biol. Chem.* **2001**, *276*, 5753−5759.
(20) Fukunaga, K.; Kobayashi, T.; Tamura, S.; Miyamoto, E. Dephosphorylation of autophosphorylated Ca^{2+}/calmodulin-dependent protein kinase II by protein phosphatase 2C. *J. Biol. Chem.* **1993**, *268*, 133−137.
(21) Desdouits, F.; Siciliano, J. C.; Nairn, A. C.; Greengard, P.; Girault, J. A. Dephosphorylation of Ser-137 in DARPP-32 by protein phosphatases 2A and 2C: different roles in vitro and in striatonigral neurons. *Biochem. J.* **1998**, *330* (Part 1), 211−216.
(22) Flajolet, M.; Rakhilin, S.; Wang, H.; Starkova, N.; Nuangchamnong, N.; et al. Protein phosphatase 2C binds selectively to and dephosphorylates metabotropic glutamate receptor 3. *Proc. Natl. Acad. Sci. U.S.A.* **2003**, *100*, 16006−16011.
(23) Das, A. K.; Helps, N. R.; Cohen, P. T.; Barford, D. Crystal structure of the protein serine/threonine phosphatase 2C at 2.0 Å resolution. *EMBO J.* **1996**, *15*, 6798−6809.
(24) Goodsell, D. S.; Olson, A. J. Automated docking of substrates to proteins by simulated annealing. *Proteins* **1990**, *8*, 195−202.
(25) Morris, G. M.; Goodsell, D. S.; Huey, R.; Olson, A. J. Distributed automated docking of flexible ligands to proteins: parallel applications of AutoDock 2.4. *J. Comput.-Aided Mol. Des.* **1996**, *10*, 293−304.
(26) Morris, G. M.; Goodsell, D. S.; Halliday, R. S.; Huey, R.; Hart, W. E.; et al. Automated docking using a Lamarckian genetic algorithm and an empirical binding free energy function. *J. Comput. Chem.* **1998**, *19*, 1639−1662.
(27) Ihlenfeldt, W. D.; Voigt, J. H.; Bienfait, B.; Oellien, F.; Nicklaus, M. C. Enhanced CACTVS browser of the Open NCI Database. *J. Chem. Inf. Comput. Sci.* **2002**, *42*, 46−57.
(28) Seidler, J.; McGovern, S. L.; Doman, T. N.; Shoichet, B. K. Identification and prediction of promiscuous aggregating inhibitors among known drugs. *J. Med. Chem.* **2003**, *46*, 4477−4486.
(29) McGovern, S. L.; Shoichet, B. K. Information decay in molecular docking screens against holo, apo, and modeled conformations of enzymes. *J. Med. Chem.* **2003**, *46*, 2895−2907.
(30) Fjeld, C. C.; Denu, J. M. Kinetic analysis of human serine/threonine protein phosphatase 2Cα. *J. Biol. Chem.* **1999**, *274*, 20336−20343.
(31) Jackson, M. D.; Fjeld, C. C.; Denu, J. M. Probing the function of conserved residues in the serine/threonine phosphatase PP2Cα. *Biochemistry* **2003**, *42*, 8513−8521.
(32) Lipinski, C. A.; Lombardo, F.; Dominy, B. W.; Feeney, P. J. Experimental and computational approaches to estimate solubility and permeability in drug discovery and development settings. *Adv. Drug Delivery Rev.* **1997**, *23*, 3−25.
(33) Veber, D. F.; Johnson, S. R.; Cheng, H. Y.; Smith, B. R.; Ward, K. W.; et al. Molecular properties that influence the oral bioavailability of drug candidates. *J. Med. Chem.* **2002**, *45*, 2615−2623.
(34) Swierczek, K.; Pandey, A. S.; Peters, J. W.; Hengge, A. C. A comparison of phosphonothioic acids with phosphonic acids as phosphatase inhibitors. *J. Med. Chem.* **2003**, *46*, 3703−3708.
(35) Iyer, S.; Younker, J. M.; Czyryca, P. G.; Hengge, A. C. A nonhydrolyzable analogue of phosphotyrosine, and related aryloxymethano- and aryloxyethano-phosphonic acids as motifs for inhibition of phosphatases. *Bioorg. Med. Chem. Lett.* **2004**, *14*, 5931−5935.
(36) Rusnak, F.; Mertz, P. Calcineurin: form and function. *Physiol. Rev.* **2000**, *80*, 1483−1521.
(37) Walsh, A. H.; Cheng, A.; Honkanen, R. E. Fostriecin, an antitumor antibiotic with inhibitory activity against serine/threonine protein phosphatases types 1 (PP1) and 2A (PP2A), is highly selective for PP2A. *FEBS Lett.* **1997**, *416*, 230−234.
(38) Mitsuhashi, S.; Matsuura, N.; Ubukata, M.; Oikawa, H.; Shima, H.; et al. Tautomycetin is a novel and specific inhibitor of serine/threonine protein phosphatase type 1, PP1. *Biochem. Biophys. Res. Commun.* **2001**, *287*, 328−331.
(39) Tatlock, J. H.; Linton, M. A.; Hou, X. J.; Kissinger, C. R.; Pelletier, L. A.; et al. Structure-based design of novel calcineurin (PP2B) inhibitors. *Bioorg. Med. Chem. Lett.* **1997**, *7*, 1007−1012.
(40) Holbeck, S. L. Update on NCI in vitro drug screen utilities. *Eur. J Cancer* **2004**, *40*, 785−793.
(41) Gasparetto, M.; Gentry, T.; Sebti, S.; O'Bryan, E.; Nimmanapalli, R.; et al. Identification of compounds that enhance the anti-lymphoma activity of rituximab using flow cytometric high-content screening. *J. Immunol. Methods* **2004**, *292*, 59−71.
(42) Guthridge, M. A.; Bellosta, P.; Tavoloni, N.; Basilico, C. FIN13, a novel growth factor-inducible serine-threonine phosphatase which can inhibit cell cycle progression. *Mol. Cell. Biol.* **1997**, *17*, 5485−5498.
(43) Tong, Y.; Quirion, R.; Shen, S. H. Cloning and characterization of a novel mammalian PP2C isozyme. *J. Biol. Chem.* **1998**, *273*, 35282−35290.
(44) Ohta, M.; Guo, Y.; Halfter, U.; Zhu, J. K. A novel domain in the protein kinase SOS2 mediates interaction with the protein phosphatase 2C ABI2. *Proc. Natl. Acad. Sci. U.S.A.* **2003**, *100*, 11771−11776.
(45) Lu, X.; Nannenga, B.; Donehower, L. A. PPM1D dephosphorylates Chk1 and p53 and abrogates cell cycle checkpoints. *Genes Dev.* **2005**, *19*, 1162−1174.
(46) Leroy, C.; Lee, S. E.; Vaze, M. B.; Ochsenbein, F.; Guerois, R.; et al. PP2C phosphatases Ptc2 and Ptc3 are required for DNA checkpoint inactivation after a double-strand break. *Mol. Cell* **2003**, *11*, 827−835.
(47) Lu, X.; Bocangel, D.; Nannenga, B.; Yamaguchi, H.; Appella, E.; et al. The p53-induced oncogenic phosphatase PPM1D interacts with uracil DNA glycosylase and suppresses base excision repair. *Mol. Cell* **2004**, *15*, 621−634.
(48) Bulavin, D. V.; Phillips, C.; Nannenga, B.; Timofeev, O.; Donehower, L. A.; et al. Inactivation of the Wip1 phosphatase inhibits mammary tumorigenesis through p38 MAPK-mediated activation of the p16-(Ink4a)-p19(Arf) pathway. *Nat. Genet.* **2004**, *36*, 343−350.
(49) Harrison, M.; Li, J.; Degenhardt, Y.; Hoey, T.; Powers, S. Wip1-deficient mice are resistant to common cancer genes. *Trends Mol. Med.* **2004**, *10*, 359−361.
(50) Bernards, R. Wip-ing out cancer. *Nat. Genet.* **2004**, *36*, 319−320.
(51) Daniel, K. G.; Gupta, P.; Harbach, R. H.; Guida, W. C.; Dou, Q. P. Organic copper complexes as a new class of proteasome inhibitors and apoptosis inducers in human cancer cells. *Biochem. Pharmacol.* **2004**, *67*, 1139−1151.
(52) Panchal, R. G.; Hermone, A. R.; Nguyen, T. L.; Wong, T. Y.; Schwarzenbacher, R.; et al. Identification of small molecule inhibitors of anthrax lethal factor. *Nat. Struct. Mol. Biol.* **2004**, *11*, 67−72.
(53) Burnett, J. C.; Schmidt, J. J.; Stafford, R. G.; Panchal, R. G.; Nguyen, T. L.; et al. Novel small molecule inhibitors of botulinum neurotoxin A metalloprotease activity. *Biochem. Biophys. Res. Commun.* **2003**, *310*, 84−93.
(54) Doman, T. N.; McGovern, S. L.; Witherbee, B. J.; Kasten, T. P.; Kurumbail, R.; et al. Molecular docking and high-throughput screening for novel inhibitors of protein tyrosine phosphatase-1B. *J. Med. Chem.* **2002**, *45*, 2213−2221.
(55) Kraemer, O.; Hazemann, I.; Podjarny, A. D.; Klebe, G. Virtual screening for inhibitors of human aldose reductase. *Proteins* **2004**, *55*, 814−823.
(56) Huang, N.; Nagarsekar, A.; Xia, G.; Hayashi, J.; MacKerell, A. D., Jr. Identification of non-phosphate-containing small molecular weight inhibitors of the tyrosine kinase p56 Lck SH2 domain via in silico screening against the pY + 3 binding site. *J. Med. Chem.* **2004**, *47*, 3502−3511.

(57) Kao, R. Y.; Jenkins, J. L.; Olson, K. A.; Key, M. E.; Fett, J. W.; et al. A small-molecule inhibitor of the ribonucleolytic activity of human angiogenin that possesses antitumor activity. *Proc. Natl. Acad. Sci. U.S.A.* **2002**, *99*, 10066−10071.
(58) Brown, J. X.; Buckett, P. D.; Wessling-Resnick, M. Identification of small molecule inhibitors that distinguish between non-transferrin bound iron uptake and transferrin-mediated iron transport. *Chem. Biol.* **2004**, *11*, 407−416.
(59) Wang, R.; Fu, Y.; Lai, L. A new atom-additive method for calculating partition coefficients. *J. Chem. Inf. Comput. Sci.* **1997**, *37*, 615−621.
(60) Willett, P. Similarity-based approaches to virtual screening. *Biochem. Soc. Trans.* **2003**, *31*, 603−606.
(61) Martin, Y. C.; Kofron, J. L.; Traphagen, L. M. Do structurally similar molecules have similar biological activity? *J. Med. Chem.* **2002**, *45*, 4350−4358.
(62) Cohen, P.; Alemany, S.; Hemmings, B. A.; Resink, T. J.; Stralfors, P.; et al. Protein phosphatase-1 and protein phosphatase-2A from rabbit skeletal muscle. *Methods Enzymol.* **1988**, *159*, 390−408.

JM051033Y